PROCEEDINGS OF SCIENCE

SiPM-based Camera Research and Development for the Wide Field of View Cherenkov Telescope Array of LHAASO

S. S. Zhang[a]*, B. Y. Bi[ab], C. WANG[a], Z. CAO[a], L. Q. YIN[ab], T. Montaruli[c], D. della Volpe[c], M. Heller[c] for the LHAASO Collaboration

[a] *Institute of High Energy Physics, CAS, Beijing, China*
[b] *University of Chinese Academy of Sciences, Beijing, China*
[c] *University of Geneva, Geneva, Switzerland*
E-mail: zhangss@ihep.ac.cn

Wide Field of View Cherenkov Telescope Array (WFCTA) of LHAASO consists of 18 air image Cherenkov telescopes. Each Cherenkov telescope consists of an array of 32×32 SiPM array which cover a field of view $14^\circ \times 16^\circ$ with a pixel size of 0.5°. The main scientific goal of WFCTA is to measure the ultra-high energy cosmic ray composition and energy spectrum from 30 TeV to a couple of EeV. Because SiPM cannot be aging under strong light exposure, SiPM-based camera can be operated in moon conditions, thus achieve a longer duty cycle than PMT-based camera, e.g. the duty cycle of SiPM-based camera is about 30%, while the PMT-based camera is about 10%. The SiPM-based camera is designed and developed for WFCTA. The square SiPM with photosensitive area of 15 mm×15 mm and Geiger-APD size of 25 μm is used to meet the required dynamic range from 10 photoelectrons (pes) to 32000 pes. Because SiPM can reach higher photon detection efficiency than quantum efficiency × collection efficiency of PMT, SiPM-based camera has almost the same signal to noise ratio with PMT-based camera of WFCTA prototype, although SiPM has higher dark count rate than PMT.

35th International Cosmic Ray Conference — ICRC2017
10–20 July, 2017
Bexco, Busan, Korea

*Speaker.

PoS(ICRC2017)423

1. Introduction

Silicon photomultipliers (SiPM) has many advantages like single photon response, high photon detection efficiency, high gain at low bias voltage, no aging due to strong light exposure and no sensitivity to magnetic fields. Therefore, the SiPM is served as the next generation of photomultiplier sensor. The next generation of Image Air Cherenkov telescopes have been exploring the use of the SiPM technology, such as the First G-APD Cherenkov Telescope [1] and the single-mirror Small Size Telescopes (SST-1M) proposed for the Cherenkov Telescope Array (CTA) project [2]. The SiPM technology is also designed and developed for the Wide Field of View Cherenkov Telescope Array (WFCTA) of the Large High Altitude Air Shower Observatory (LHAASO) [3, 4]. WFCTA consists of 18 Cherenkov telescopes. Each Cherenkov has a field of view (FOV) of $14^\circ \times 16^\circ$ with a pixel size of approximately $0.5^\circ \times 0.5^\circ$. A 5 m^2 spherical aluminized mirror made of 20 hexagonal mirrors and 5 half hexagonal mirrors are used for each telescope. The main scientific goal of WFCTA is to measure the ultra-high energy cosmic ray composition and energy spectrum from 30 TeV to a couple of EeV. The portable design of the telescope is dedicated to enable an easy switching between configurations of the array in order to carry out spectrum and composition measurements of cosmic rays in different energy ranges. WFCTA observes the primary cosmic ray energy more than 2.5 orders in each observation mode, which requires the dynamic range of each pixel between 10 photoelectrons (pes) and 32000 pes. SiPM-based camera can operate in moon conditions and achieves a longer duty cycle than PMT-based camera. The design and the performance of the SiPM-based camera will be described in detail in the paper.

2. SiPM candidates

The SiPM is made of an avalanche photodiode (APD) array. Each APD in SiPM operates in Geiger-mode and is coupled with a quenching resistor. The APD size can vary from 15 μm to 100 μm. The density of SiPM is 1600 APDs/mm^2 for 25 μm APD size. All the APDs in the SiPM can be read in parallel making it possible to generate signals with a dynamic range from 1 pe to a few hundred pes per 1 mm^2 photosensitive area. The saturation happens when two or more photons hit on the same APD at same time. So, the dynamic range of SiPM is proportional to the total number of APD cells in SiPM and dependent on the light distribution hitting on the SiPM. As shown in Fig. 1(a), the SiPM dynamic range measured results can be fitted very well by the function which describes the relationship between the number of fired APDs and the total number of APDs in the SiPM. A larger dynamic range requires more total number of APDs. Larger area SiPM has a bigger dark count rate (DCR) and the smaller APD size will produce smaller fill factor and then smaller photon detection efficiency (PDE). After taking these factors into account, the square SiPM with photosensitive area of 15 mm$\times$15 mm and APD size of 25 μm is selected. We have evaluated the SiPM candidates from Hamamatsu, FBK and SensL[6]. The 15 mm$\times$15 mm SiPM with APD size 25 μm can reach the dynamic range from 10 pes to 32,000 pes. The additional deviation from the non-uniform light distribution caused by the light concentrator and the spherical mirror is less than 2% at 32000 pes. The parameters of SiPM candidates from Hamamatsu, FBK and SensL are shown in Table 1. FBK and SensL SiPM candidates have a higher fill factor, so their SiPM candidates have a higher PDE. Accordingly, DCR and optical cross talk (OCT) of FBK

and SensL SiPM candidates is higher than that of Hamamatsu SiPM candidates. The response of a Hamamatsu SiPM candidate in low photons intensity is shown Fig. 2(a) and the response of a FBK SiPM candidate in low photons intensity is shown in Fig. 2(b). The photons can be counted visibly when the SiPMs exposure in the low photons intensity. The single photon response of Hamamatsu SiPM is better than FBK SiPM, because Hamamatsu SiPM has lower DCR than FBK SiPM. The resolution of the SiPM is shown in Fig. 1(b). The resolution of the SiPM is worse than Poisson expectation resolution, the main reason is that DCR of the SiPM is very high. The resolution of the SiPM is better than 5% at 1000 pes, which meets the requirements of WFCTA.

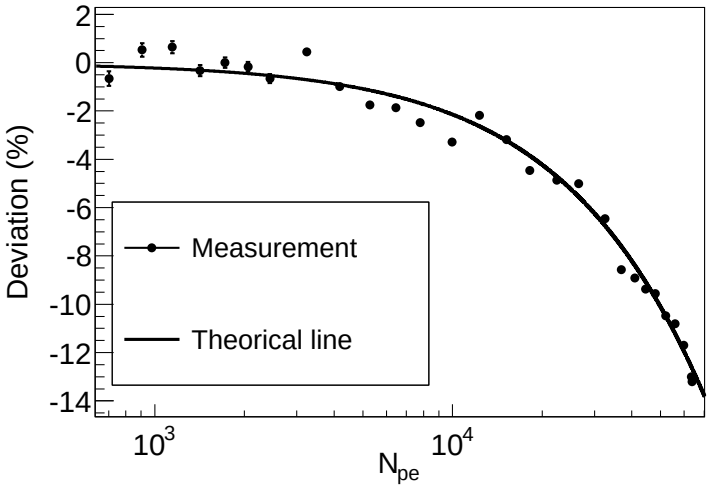

(a)

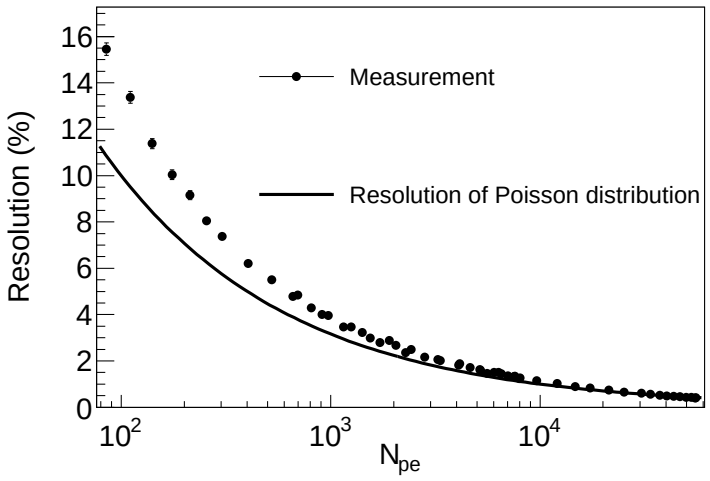

(b)

Figure 1: (a) The SiPM dynamic range measured results (black dot) can be fitted very well by the function (black line) which describes the relationship between the number of fired APDs and the total number of APDs in the SiPM. (b) The resolution of SiPM: measurement results (black dot) and Poisson expectation (black line).

Table 1: The parameters of SiPM candidates from Hamamatsu, FBK and SensL.

Candidates	Hamamatsu	FBK	SensL
PDE@400nm	25%	38%	33%
Fill factor	47%	72%	62%
Dark count rate	$45kHz/mm^2$	$80kHz/mm^2$	$80kHz/mm^2$
Optical cross talk	1%	15%	5%
Gain (10^6)	0.7	1.38	1.70
Break down voltage	51.8 V	26.5 V	24.5 V
Break down voltage vs. temperature	$54mv/^\circ C$	$26mv/^\circ C$	$21.5mv/^\circ C$
Gain vs. temperature	$1.5\%/^\circ C$	$1.5\%/^\circ C$	$1.5\%/^\circ C$

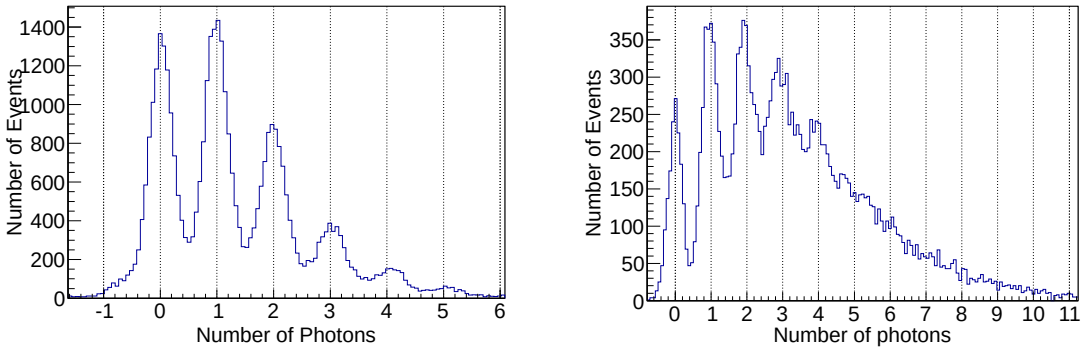

(a) (b)

Figure 2: (a) The response of a Hamamatsu SiPM candidate in low photons intensity. (b) The response of a FBK SiPM candidate in low photons intensity.

3. SiPM-based camera

Each SiPM-based camera consists of an array of 32×32 SiPM and readout electronics. Firstly, SiPM signals are fed to pre-amplifiers through a direct current (DC) coupling (Fig. 3(a)). The intensity of the sky background light can be monitored directly under the DC coupling design. A bright star can be measured by the telescope and is used to calibrate the direction of the telescope when the star passed through the FOV of the telescope [5]. A typical signal out of pre-amplifier is shown in Fig. 3(b). The signal width is about 50 ns. Secondly, signals coming out of the pre-amplifiers are split into two channels and are amplified by two chains of amplifier: high gain and low gain separately for getting a good linearity over a wide dynamic range of 3.5 orders of magnitude in charge. And then the signals are digitized by 50-MHz, 14 bits flash analog-to-digital-converters (FADCs). Finally, the digital signals are collected by FPGAs to do further processing: single channel trigger, event trigger, signals transmission and storage etc. The architecture of SiPM camera readout electronics is shown in Fig. 4. The SiPM gain or break down voltage is sensitive to the temperature. The SiPM gain change about 1.5% per centigrade degree, or the break down voltage change about 26 mv for FBK SiPM, 21.5 mv for SensL SiPM and 54 mv for Hamamatsu SiPM per centigrade degree. A temperature and high voltage compensation loop is used to keep

the SiPM gain stable.

Each SiPM-based camera are grouped into 64 sub-clusters. Each sub-cluster (Fig. 6(a)) consists of 16 light concentrators (Winston cone), 16 SiPMs (temperature sensor is embedded in the SiPM chip), a pre-amplifier board, a slow control board (16 temperature and high voltage compensation loops), two analogue board (each board has 8 channels of high gain and low gain amplifier chains) and a digital board (including 32 50 MHz, 14 bits FADCs and a FPGA). The pixel size of the camera is 25.8 mm×25.8 mm. Each pixel is a SiPM with photosensitive area of 15 mm×15 mm. Light concentrators are used to guide the photons hitting on the non-photosensitive area into photosensitive area (see Fig. 5(a) and Fig. 5(b)). The inlet size of the light concentrator is matched to the pixel size and the outlet size of the light concentrator is matched to the SiPM photosensitive area. The photon collection efficiency is about 34% without the light concentrator and increases to 81% with the light concentrator. Most of sky background light wavelength are higher than 550 nm in the moon less night [8]. The PDE of SiPM is about 30% at 550 nm and 3% at 900 nm. So an optical filter window with cutoff wavelength of 550 nm is mounted in the front of the SiPM-based camera (see Fig. 6(b)), which is used to improve the signal to noise ratio of the camera. An air internal recycling cooling system is used to cool the SiPM-based camera. In order to ensure the uniformity of temperature distribution in the camera as much as possible, each SiPM-based camera has two air inlets and two air outlets on two sides of the camera (see Fig. 6(b)). The reflectivity of the light concentrator is very sensitive to the dust. So, the whole system is sealed to prevent outside dust from entering.

The PDE of SiPM is about two times of PMT's quantum efficiency × collection efficiency (ε·Qe). The dark count rate of 15 mm×15 mm SiPM is about 18 MHz at 0.5 pe threshold and the dark count rate of PMT is less than 10 kHz at 0.5 pe threshold. The sky background noise is related to the intensity of the sky background light and the PDE/ε·Qe of the SiPM/PMT. The sky background noise at the YangBaJing Cosmic Ray Observatory [6] is about 49 MHz for SiPM and 24 MHz for the PMT at the moonless night. Because SiPM has higher PDE than ε·Qe of PMT, compared with PMT-based camera of WFCTA prototype [6], SiPM has the same or even higher signal-to-noise ratio, although SiPM has higher dark count rate than PMT. The energy threshold of the telescope will increase when the sky background noise increase, e.g. the energy threshold is about 30 TeV at moon less night and the energy threshold is about 300 TeV at half-moon night.

4. Gain monitoring

Six UV-LEDs (400 nm) are mounted at the center of the mirror, which are used to monitor and calibrate the gain the SiPM-based camera. A diffuser is put in front of the LED and nearly uniform LED light are expected to hit on every pixel in the camera. The photons intensity of six UV-LEDs is about 1000 pes with pulse width less than 20 ns. A resistor R_0=200 Ω in the Fig. 3(a) is used to protect the SiPM from damage under the strong light condition. The voltage drop on the R_0 (V_{R_0}) varies with the intensity of the sky background light. Accordingly, the supply voltage or the gain of the SiPM varies with the intensity of the sky background light, because the supply voltage of the SiPM is equal to V_{cc}-V_{R_0}. So, one LED with 1 Hz frequency is used to monitor the gain of the camera every minute. The LED is also used to monitor the temperature and high voltage compensation loop which is used to keep the SiPM gain stable in the case of environmental

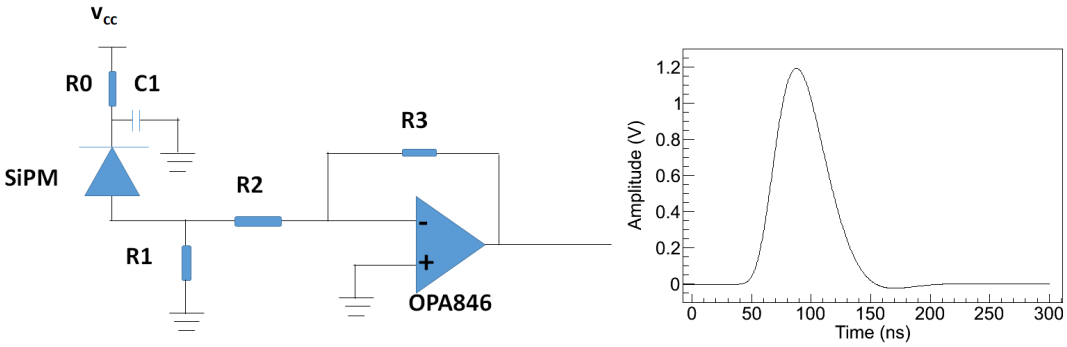

Figure 3: (a) SiPM readout and pre-amplifier schematic. (b)A typical SiPM signal from a pre-amplifier with a pulse width of about 50 ns.

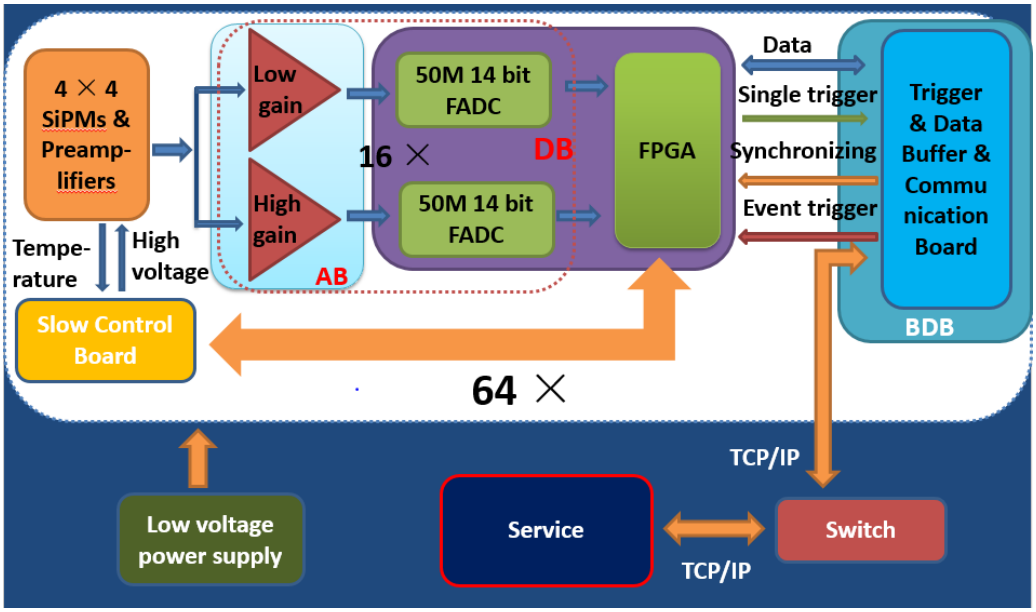

Figure 4: The architecture of SiPM camera readout electronics.

temperature changes. Three LEDs: LED A, LED B and LED C with 50 Hz frequency are used to calibrate the gain of the camera before the observation and after the observation. Firstly, LED A, LED B and LED C are measured by high gain channels of the camera respectively. And then LED A, LED B and LED C emit light simultaneously and is measured by low gain channels of the camera. The absolute LED light intensity can be calibrated with uncertainty less than 7% [6]. Six UV-LEDs are calibrated by the same absolute calibration device. The uncertainty of the difference between six UV-LEDs is expected to be zero. High gain channels and low gain channels are calibrated separately, which can avoid the deviation caused by the electronics and the SiPM transfer from high gain channels to low gain channels. High gain channels cover the dynamic range between 10 pes and 1300 pes. Low gain channels cover the dynamic range between 250 pes and 32000 pes. The monitoring points (about 1000 pes) for high gain channels and the monitoring points (3000

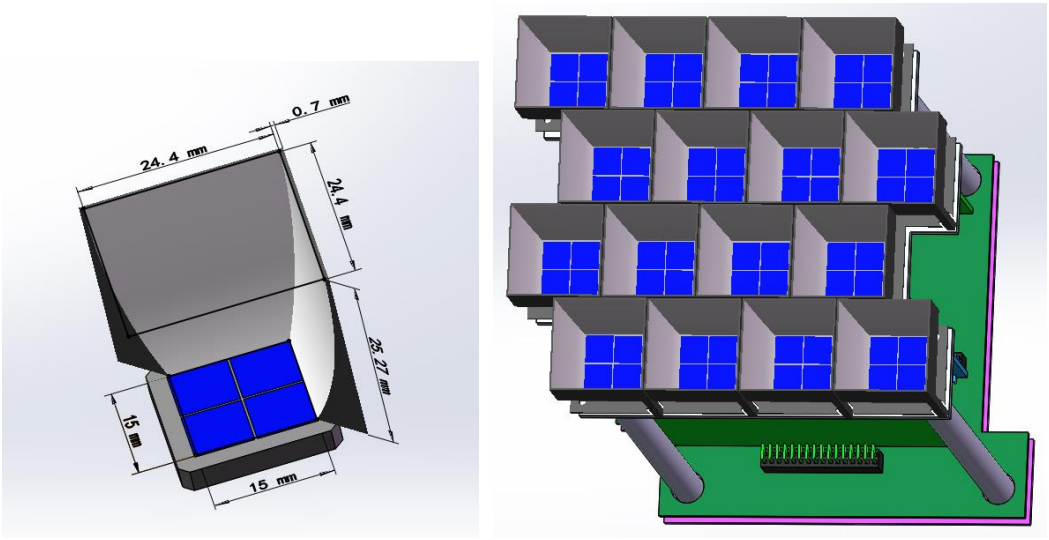

(a) (b)

Figure 5: (a) The shape of half light concentrator with the dimensions indicated and the SiPM shown in the bottom of light concentrator. (b) A front view of a sub-cluster.

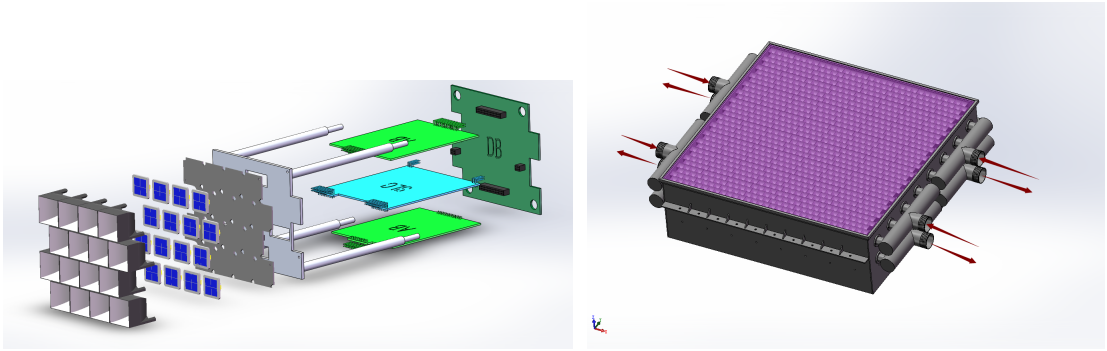

(a) (b)

Figure 6: (a) A sub-cluster assembly explosion diagram. (b) A SiPM-based camera design picture.

pes) for low gain channels have a relative deviation less than 1%. The LED will age after emitting light for a long time. The remaining two LEDs are used to monitor the above four LEDs. The remaining two LEDs calibrate the other four LEDs two times a month and the six UV-LEDs are calibrated again by the absolute calibration device every year.

5. Discussion and Conclusion

SiPM-based camera are designed to meet the requirements of LHAASO-WFCTA. SiPM-based camera can be operated on moon nights and achieve a longer duty cycle than PMT-based camera. The duty cycle of SiPM-based camera is expected to be more than 30%. The signal-to-noise ratio of SiPM-based camera is the same as PMT-based camera of WFCTA prototype [6]. The energy threshold of LHAASO-WFCTA is about 30 TeV at moon less night and is less than 300 TeV at

half-moon night. The 15 mm$\times$15 mm SiPM with APD size 25 μm can reach the dynamic range from 10 pes to 32,000 pes and meets the requirements of LHAASO-WFCTA . The gain monitoring system is designed to monitor the gain of the camera during the observation. The first prototype of SiPM-based camera will be built at the beginning of 2018 and the 6 SiPM-based telescopes are expected to run at LHAASO site at the end of 2018.

6. Acknowledgements

This work is supported in China by the Key Laboratory of Particle Astrophysics, Institute of High Energy Physics, CAS. Projects No. 11475190 and No. 11675204 of NSFC also provide support to this study.

References

[1] H. Anderhub et al., Design and Operation of FACT - The First G-APD Cherenkov Telescope, JINST 8 P06008, 2013, arXiv:1304.1710

[2] E. J. Schioppa et al., The SST-1M camera for the Cherenkov Telescope Array, arXiv:1508.06453v1 [astro-ph.IM], 2015

[3] Z. Cao et al., Chinese Physics C 34, 249 (2010)

[4] H.H. He et al., LHAASO Project: detector design and prototype, 31st ICRC, LODZ, (2009)

[5] MA Ling-Ling et al., Chinese Physics C 35(5), 478 (2011)

[6] S.S. Zhang et al., Nucl. Instr. and Meth. A 629, 57 (2011)

[7] B.Y. Bi et al., Studies of Silicon Photomultipliers and Preamplifier for the Wide Field of View Cherenkov Telescope Array of LHAASO, in Proceedings of 35th International Cosmic Ray Conference, Bexco, Busan, Korea (2017)

[8] C.R. Benn, S.L. Ellison, New Astronomy Reviews 42, 503 (1998)